Check for updates

A series of lanthanide glutarates: lanthanide contraction effect on crystal frameworks of lanthanide glutarates†

Xiao-Feng Tan,[a] Jian Zhou, [ID] *[a] Hua-Hong Zou,*[b] Lianshe Fu,*[c] Qiuling Tang[a] and Peng Wang[a]

A series of lanthanide glutarates [Ln(phen)(glu)Cl]$_n$ {Ln = Y (**1a**), Tm (**1b**); phen = 1,10-phenanthroline; glu = glutarate}, [Ln$_2$(phen)$_2$(glu)$_3$]$_n$ {Ln = Ce (**2a**), Tb (**2b**), Ho (**2c**)} and [La$_2$(glu)$_3$(H$_2$O)$_3$]$_n$·5nH$_2$O (**3**) have been hydrothermally synthesized and characterized structurally. Compounds **1a–b** are isostructural and consist of 1-D neutral [Ln(phen)(glu)Cl]$_n$ chains, which are built up from the linkages of [Ln(phen)Cl]$^{3+}$ ions and glutarate ligands. Compounds **2a–c** are isostructural and contain 2-D [Ln$_2$(phen)$_2$(glu)$_3$]$_n$ layers, where Ln^{3+} ions are connected by three kinds of glutarate ligands. The 3-D framework of compound **3** is constructed by the linkages of La^{3+} ions and glutarate ligands. Although some 3-D lanthanide glutarates have been reported, they exhibit a very robust structural type, whose structure is not changed by different Ln^{3+} ions, but compound **3** shows a new structural type. A systematic investigation of six lanthanide glutarates and some reported compounds revealed that the well-known lanthanide contraction has a significant influence on the formation of lanthanide glutarates. The photoluminescent properties of **1b** and **2b**, and magnetic properties of **1b**, **2b** and **2c** have been studied.

Introduction

Lanthanide coordination polymers are of great interest due to their fantastic topological structures, and potentially applicable magnetic and photoluminescence properties.[1] The magnetic properties could arise from the intrinsic large spin ground state and the strong uniaxial magnetic anisotropy of some trivalent lanthanide ions (Ln^{3+}),[2] while the luminescence of Ln^{3+} ions is possible from intra-configurational f–f transitions, which show fascinating luminescence in the visible or near-infrared spectral regions upon irradiation with ultraviolet radiation.[3] Due to the low absorption of the forbidden f–f transitions, the emissions of Ln^{3+} ions are weak. In order to enhance the emissive efficiency and decrease the internal non-radiative decay processes, two strategies may be generally utilized. One is to prevent water molecules from binding to Ln^{3+} ions, as well as high-vibrational

O–H, N–H and C–H oscillators that tend to quench photoluminescence,[4] the other is to promote the antenna effect, which pumps up Ln^{3+} emission by using π-conjugated organic aromatic chromophores directly coordinated to Ln^{3+} ions.[5] Bidentate neutral 1,10-phenanthroline (phen) is one of the widest used chromophoric ligand in the design of photoluminescent lanthanide complexes, because it can chelate to Ln^{3+} ion, which may not only encapsulate and protect the Ln^{3+} ion from the water molecules, but also absorb and efficiently transfer energy onto the Ln^{3+} excited states. As expected, a large number of photoluminescent Ln-complexes containing neutral phen and its derivatives have been synthesized,[6] but their solids are difficult to directly use as photoluminescent sources, mainly because phen or its derivatives acting as terminating group prevent further connections, resulting in molecules that show poor thermal stability, weak moisture stability and feeble mechanical strength.

Glutaric acid is one of excellent long-chain aliphatic dicarboxylic acids with flexible bridging capability for the construction of a diversity of lanthanide coordination polymers.[7] But water molecule is easily bound to Ln^{3+} ion in the absence of chelating chromophoric ligand, which could lead to efficient nonradiative deactivation of their excited states. It is expected that phen or its derivatives in conjunction with glutaric acid may generate a new class of lanthanide coordination polymers with enhanced thermal stability, high luminescence quantum yield and relatively long-lived emission. However, a few

[a] College of Chemistry, Chongqing Normal University, Chongqing, 401331, P. R. China. E-mail: jianzhou888888@163.com

[b] State Key Laboratory for Chemistry and Molecular Engineering of Medicinal Resources, School of Chemistry & Pharmacy of Guangxi Normal University, Guilin, 541004, P. R. China

[c] Department of Physics and CICECO-Aveiro Institute of Materials, University of Aveiro, 3810-193, Aveiro, Portugal

lanthanide glutarates containing phen or its derivatives were prepared under certain synthetic conditions,[8] where the significant influence of lanthanide contraction on their structures and the relationship between the structures and photoluminescent properties have been rarely reported to the best of our knowledge. To further explore the influences on the formation of lanthanide glutarates, it is necessary to synthesize a series of new lanthanide glutarates for improving their desirable photoluminescent properties. This paper reports the synthesis, crystal structures and properties of a series of new lanthanide glutarates $[Ln(phen)(glu)Cl]_n$ {Ln = Y (1a), Tm (1b)}, $[Ln_2(phen)_2(glu)_3]_n$ {Ln = Ce (2a), Tb (2b), Ho (2c)} and $[La_2(glu)_3(H_2O)_3]_n \cdot 5nH_2O$ (3). A systematic investigation of six lanthanide glutarates and some reported compounds exhibited that the well-known lanthanide contraction has a significant influence on the formation of lanthanide glutarates.

Experimental

General remarks

All analytical grade chemicals were obtained commercially and used without further purification. IR spectra were obtained from a powdered sample pelletized with KBr on an ABB Bomen MB 102 series IR spectrophotometer in the range of 400–4000 cm^{-1}. Elemental analyses (C, H, N) were performed on an Elemental Vario EL III analyzer. The photoluminescence spectra were recorded at room temperature with a modular double grating excitation spectrofluorimeter with a TRIAX 320 emission monochromator (Fluorolog-3, Horiba Scientific) coupled to an R928 Hamamatsu photomultiplier. The excitation source was a 450 W Xe arc lamp. The emission spectra were corrected for detection and optical spectral response of the spectrofluorimeter and the excitation spectra were corrected for the spectral distribution of the lamp intensity using a photodiode reference detector. Variable-temperature magnetic susceptibility measurements were carried out in the temperature range of 2–300 K with a Quantum Design MPMS-5 magnetometer. Thermogravimetric analyses (TGA) were performed using a Mettler TGA/SDTA851 thermal analyzer under an air-flow atmosphere with a heating rate of 10 °C min^{-1} in the temperature region of 25–600 °C.

Synthesis of Y(phen)(glu)Cl]$_n$ (1a)

A mixture of glutaric acid (0.0264 g, 0.20 mmol), phen (0.0270 g, 0.15 mmol), YCl_3 (0.0742 g, 0.38 mmol), and water (2 mL) was stirred for 1 h, and then the pH value of the mixed solution was adjusted to 5–6 by triethylamine. The final mixture was sealed in a 25 mL Teflon lined autoclave and heated at 100 °C for 7 days. After cooling to room temperature slowly, colorless block crystals were isolated. The yield of 1a is 73% based on YCl_3. Anal. calcd for 1a, $C_{17}H_{14}ClN_2O_4Y$, C 46.98%, H 3.25%, N 6.44%, found: C 47.12%, H 3.28%, N 6.47%. IR (cm^{-1}): 3094(w), 3054(w), 2900(w), 1598(s), 1517(w), 1420(s), 1350(m), 1280(m), 1219(m), 1169(m), 1099(m), 1059(m), 934(vw), 859(s), 817(m), 781(m), 727(s), 650(m), 539(w).

Synthesis of Tm(phen)(glu)Cl]$_n$ (1b)

The colorless crystals of 1b were prepared similarly from $TmCl_3$ (yield 63% based on $TmCl_3$). Anal. calcd for 1b, $C_{17}H_{14}ClN_2O_4Tm$, C 39.67%, H 2.74%, N 5.44%, found: C 39.63%, H 2.76%, N 5.46%. IR (cm^{-1}): 3094(w), 3054(w), 2900(w), 1591(vs), 1517(w), 1467(w), 1413(s), 1350(m), 1280(m), 1212(m), 1156(m), 1106(m), 1052(m), 962(vw), 851(s), 817(m), 781(m), 727(s), 664(m), 540(w).

Synthesis of $[Ce_2(phen)_2(glu)_3]_n$ (2a)

The yellow crystals of 2a were prepared similarly from $CeCl_3$ (yield 78% based on $CeCl_3$). Anal. calcd for 2a, $C_{39}H_{34}Ce_2N_4O_{12}$, C 45.44%, H 3.32%, N 5.43%, found: C 45.46%, H 3.34%, N 5.47%. IR (cm^{-1}): 3081(w), 3040(w), 2923(w), 1598(vs), 1524(s), 1426(s), 1343(m), 1316(s), 1266(m), 1142(m), 1106(m), 1059(m), 857(s), 794(s), 734(s), 677(w), 636(m), 519(m).

Synthesis of $[Tb_2(phen)_2(glu)_3]_n$ (2b)

The brown crystals of 2b were prepared similarly from $TbCl_3$ (yield 73% based on $TbCl_3$). Anal. calcd for 2b, $C_{39}H_{34}N_4O_{12}Tb_2$, C 43.84%, H 3.21%, N 5.24%, found: C 43.86%, H 3.23%, N 5.28%. IR (cm^{-1}): 3013(w), 2894(w), 1544(s), 1454(s), 1413(s), 1350(m), 1280(m), 1219(m), 1183(w), 1065(m), 1009(w), 934(w), 885(m), 824(m), 740(s), 664(m), 520(m).

Synthesis of $[Ho_2(phen)_2(glu)_3]_n$ (2c)

The red crystals of 2c were prepared similarly from $HoCl_3$ (yield 83% based on $HoCl_3$). Anal. calcd for 2c, $C_{39}H_{34}Ho_2N_4O_{12}$, C 43.35%, H 3.17%, N 5.18%, found: C 43.37%, H 3.19%, N 5.21%. IR (cm^{-1}): 3094(w), 3047(w), 2930(w), 1627(s), 1551(s), 1440(s), 1350(m), 1316(m), 1266(m), 1149(m), 1106(m), 1065(m), 851(s), 808(m), 734(s), 670(w), 643(m), 536(m).

Synthesis of $[La_2(glu)_3(H_2O)_3]_n \cdot 5nH_2O$ (3)

The colorless crystals of 3 were prepared similarly from La_2Cl_3 (yield 67% based on La_2Cl_3). Anal. calcd for 3, $C_{15}H_{34}La_2O_{20}$, C 22.18%, H 4.22%, found: C 22.23%, H 4.27%. IR (cm^{-1}): 3435(s), 2950(w), 1551(s), 1440(s), 1323(m), 1259(m), 1169(w), 1072(w), 968(m), 885(m), 801(w), 657(m), 546(m).

X-ray crystallography

Single-crystal X-ray diffraction data for all compounds were collected on a Rigaku Mercury CCD diffractometer using a ω-scan method with graphite monochromated Mo Kα radiation ($\lambda = 0.71073$ Å). Routine Lorentz polarization and absorption corrections were applied using multi-scan technique. The structures of all compounds were solved by direct methods of SHELXS-97 (ref. 9) and refined by full-matrix least-squares methods on F^2 using the SHELXL-97 program package.[10] Positions of H atoms from phen and glu ligands were geometrically placed and H atoms were refined isotropically as a riding mode using the default SHELXTL parameters. A summary of crystallographic data is listed in Table 1. 1528897–

Table 1 Crystallographic data for all compounds

	1a	1b	2a	2b	2c	3
Formula	$C_{17}H_{14}ClN_2O_4Y$	$C_{17}H_{14}Cl\,N_2O_4Tm$	$C_{39}H_{34}Ce_2N_4O_{12}$	$C_{39}H_{34}N_4O_{12}Tb_2$	$C_{39}H_{34}Ho_2N_4O_{12}$	$C_{15}H_{34}La_2O_{20}$
F_w	434.66	514.68	1030.94	1068.56	1080.56	812.24
Crystal system	Monoclinic	Monoclinic	Triclinic	Triclinic	Triclinic	Triclinic
Space group	$P2_1/n$	$P2_1/n$	$P\bar{1}$	$P\bar{1}$	$P\bar{1}$	$P\bar{1}$
a, Å	8.1640(4)	8.1381(11)	8.8586(18)	8.7895(4)	8.7671(5)	9.076(2)
b, Å	12.4878(6)	12.4629(16)	13.565(3)	13.4391(7)	13.4002(7)	9.867(3)
c, Å	16.1848(8)	16.161(3)	16.392(3)	16.4098(9)	16.4124(11)	16.303(4)
α, deg	90	90	84.12(3)	83.909(2)	83.911(2)	103.349(16)
β, deg	94.013(2)	94.034(5)	83.86(3)	84.340(2)	84.424(2)	104.110(9)
γ, deg	90	90	75.14(3)	74.984(2)	75.048(2)	98.526(10)
V, Å^3	1646.00(14)	1635.1(4)	1887.2(7)	1856.50(16)	1847.46(19)	1345.0(6)
Z	4	4	2	2	2	2
T, K	293(2)	297(2)	293(2)	300(2)	297(2)	293(2)
Calcd density, Mg m^{-3}	1.754	2.092	1.814	1.912	1.942	2.006
$F(000)$	872	992	1016	1044	1052	796
2θ (max), deg	50.20	50.80	36.06	50.20	50.20	50.20
Total reflns collected	134 409	9275	14 486	18 336	17 479	49 759
Unique reflns	2927	2967	2610	6573	6519	4781
R_1 [$I > 2\sigma(I)$]	0.0402	0.0429	0.0242	0.0334	0.0342	0.0281
wR_2 (all data)	0.1311	0.0719	0.0582	0.0561	0.0532	0.0791

1528902 contains the supplementary crystallographic data for this paper.†

Results and discussion

Crystal structure

Description of [Ln(phen)(glu)Cl]$_n$ [Ln = Y (1a), Tm (1b)]. Both **1a** and **1b** are isostructural, so only **1a** is discussed here in detail. **1a** crystallizes in the monoclinic space group $P2_1/n$ with four formula units in the unit cell. The asymmetric unit contains one Y^{3+} ion, one glu ligands and one phen ligand (Fig. S1†). The coordination geometry of Y^{3+} ions is a distorted triangular dodecahedron comprised of five O atoms from four glu ligands, two N atoms of one chelating phen ligand and one Cl$^-$ ion. The Y–O/N bond distances vary from 2.270(4) to 2.550(4) Å, and the Y–Cl bond length is 2.6287(15) Å, which are in agreement with corresponding values in other Y^{3+} complexes.[11] The glu ligand with an *anti–gauche* conformation adopts chelating/bridging tridentate and bridging bidentate mode, which are connected with Y^{3+} ions to form 1-D chain (Fig. 1a). Phen ligands are regularly appended to both sides of the chain. These chains are arranged in a parallel manner and further extended *via* π–π aromatic stacking interactions between phen ligands of adjacent chains with centroid-to-centroid distances of 3.633 Å to generate a 2-D layer (Fig. 1b). Then 2-D layers are interconnected into a 3-D H-bond network structure *via* C–H⋯Cl and C–H⋯O H-bonds (Fig. S2†). The C⋯O distances are in the range of 2.951(6)–3.295(5) Å and the C–H⋯O angles are in the range of 123–150°. The C⋯Cl distances vary from 3.686(5) to 3.705(6) Å and the C–H⋯Cl angles vary from 158 to 166°.

Description of [Ln$_2$(phen)$_2$(glu)$_3$]$_n$ {Ln = Ce (2a), Tb (2b), Ho (2c)}. Compounds **2a–c** are isostructural. Therefore, only **2a** is discussed here in detail. **2a** crystallizes in the triclinic space group $P\bar{1}$. The asymmetric unit contains two Ce^{3+} ions, three glu ligands and two phen ligands (Fig. S3†). The coordination geometry of each Ce^{3+} ion can be described as a distorted capped trigonal antiprism comprised of seven O atoms of five glu ligands and two N atoms of phen ligand. The Ce–O/N bond lengths are 2.4208(12)–2.7425(15) Å, which are compared with those in other Ce^{3+} complexes containing carboxylate groups and phen ligands.[12] There are three crystallographically distinct
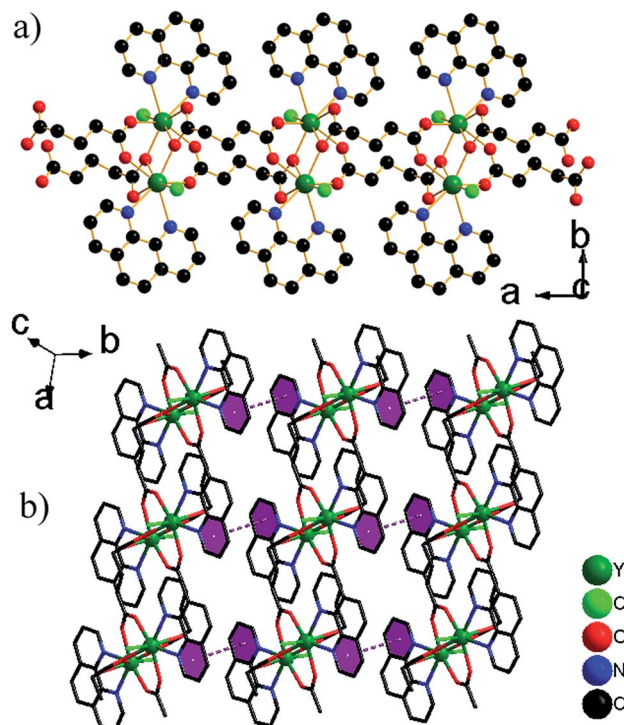

Fig. 1 (a) 1-D chain in **1a**. (b) Part of the crystal structure of **1a**, showing the formation of a layer constructed by π–π stacking interactions. H atoms bonded to C/N atoms have been omitted for clarity.
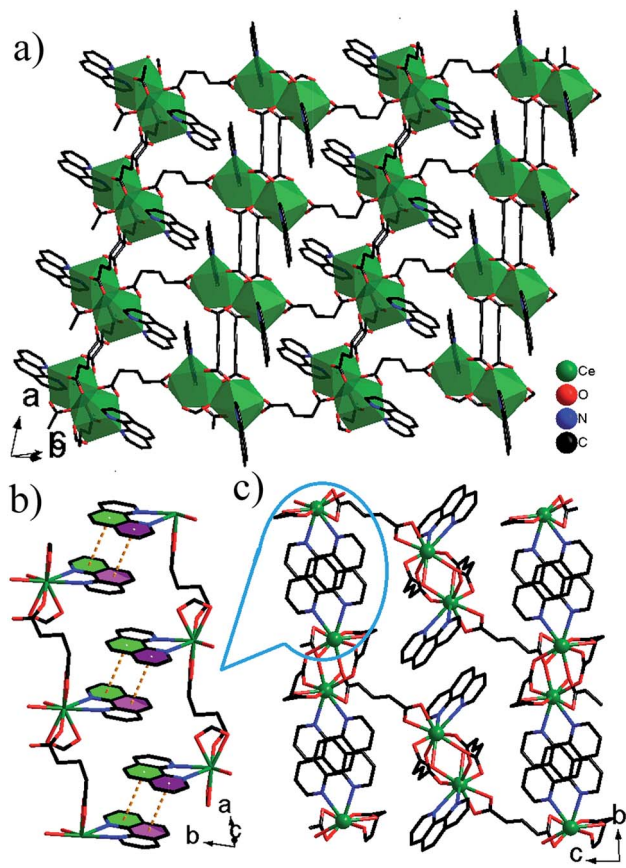
Fig. 2 (a) 2-D layer in **2a**. (b) 3-D network structure in **2a**. (c) π–π stacking interactions between phen ligands. H atoms bonded to C/N atoms have been omitted for clarity.

Fig. 3 (a) The asymmetric unit of **3**. (b and c) The coordination environments of La^{3+} ions. (d–f) Coordination modes of glu ligand in **3**. (g) 2-D layer. View of the 3-D framework in **3** along the [100] (h) and [001] (i) directions. H atoms bonded to C atoms have been omitted for clarity.

glu ligands, which exhibit two different conformations, namely *anti–anti* and *anti–gauche*. One adopts *anti–anti* conformation, illustrated by the C6–C7–C8–C9 [178.22(4)°] and C7–C8–C9–C10 [178.84(4)°] torsion angles, the other adopt the distorted *anti–gauche* conformation demonstrated by the C1–C2–C3–C4 [63.82(6)°] or C11–C12–C13–C14 [62.48(5)°] torsion angles, and C2–C3–C4–C5 [172.85(4)°] or C12–C13–C14–C15 [176.58(4)°] torsion angles, respectively. The Ce^{3+} ions are grouped in pairs by bridging carboxylate O atoms. Each pair is connected to four neighbouring pairs *via* glu ligands, resulting in network of (4,4) topology with the total Schläfli symbol of $4^4 \cdot 6^2$ and the long vertex symbol of $4 \cdot 4 \cdot 4 \cdot 4$ (Fig. 2a). A 3-D network structure is formed by π–π stacking interactions between phen ligands in the adjacent layers with mean centroid-to-centroid distances of 3.726 Å (Fig. 2b–c).

Description of [La$_2$(glu)$_3$(H$_2$O)$_3$]$_n$·5nH$_2$O (3). Although phen in **3** was not incorporated into the final structure, experiments conducted so far show that **3** cannot be synthesized in the absence of phen. So phen played an important role in the formation of **3**, but the mechanism of the reaction is still unclear. **3** crystallizes in the triclinic space group $P\bar{1}$. The asymmetric unit contains two La^{3+} ions, three glu ligands, three coordinated H$_2$O molecules and five free H$_2$O molecules (Fig. 3a). The La(1)$^{3+}$ ion adopts a tetracapped trigonal prism with eight O atoms of four glu ligands and two H$_2$O molecules
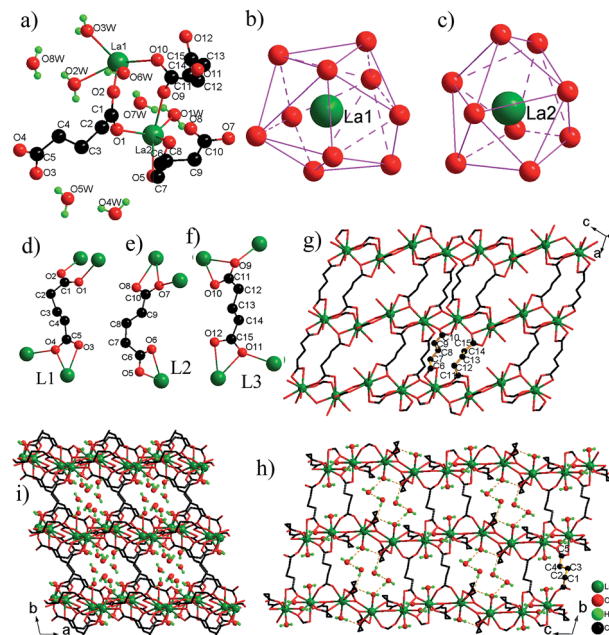
(Fig. 3b), while the La(2)$^{3+}$ ion adopts a monocapped dodecahedron with eight O atoms of six glu ligands and one H$_2$O molecules (Fig. 3c). The La–O bond distances are in the range from 2.463(3) Å to 2.897(3) Å. There are three kinds of coordination modes of glu ligands with the *anti–gauche* conformation in **3** (Fig. 3d–f). The first type (L1) is one chelating–*anti* and one *anti–syn* COO ends. The second type (L2) is one chelating and one chelating–*anti* COO ends. The third type (L3) is one chelating–*anti* and one chelating–*anti* COO ends. La(1)$^{3+}$ and La^{3+} ions are bridged by two –COO groups in the *anti–syn* mode from two glu ligands and one –COO group in the chelating–*anti* mode from one glu ligand to La$_2$ dimer with a La⋯La distance of 4.301(1) Å. The La$_2$ dimer units are interconnected *via* chelating–*anti* –COO groups to produce a 1-D infinite chain, which is further connected by ligands L2 and L3 into a layer parallel to the (010) plane (Fig. 3g). These layers are pillared by ligand L1 with its chelating–*anti* –COO group connecting one layer, and its *anti–syn* –COO group connecting the adjacent layer, leading to a novel 3-D network structure with the 1-D channels occupied by free water molecules (Fig. 3h–i). There are a lot of O–H⋯O H-bonds between the coordinated H$_2$O molecules and O atoms of –COO– groups, which play an important role in stabilizing **3** in the solid state. Moreover, the coordinated H$_2$O and free H$_2$O molecules interact also by O–H⋯O H-bonds, resulting in the formation of chain-like (H$_2$O)$_3$ unit and (H$_2$O)$_4$ ring (Fig. S4†), which are retained within the 1-D channels. The O⋯O distances are in the range of 2.746(5)–2.946(5) Å and the O–H⋯O angles vary from 143.7 to 177.6°, and are consistent with the values reported in the literature.[7]

Although 3-D frameworks of **3** and reported lanthanide glutarates $[Ln(glu)_3(H_2O)_2]_n \cdot 4nH_2O$ [Ln = Pr (**4a**), Nd (**4b**), Sm (**4c**), Eu (**4d**), Gd (**4e**), Dy (**4f**), Ho (**4g**) and Y (**4h**)][7a–c] are built from Ln^{3+} ions and glu ligands, the structures are completely different: (a) different 1-D inorganic chains: 1-D chains of **4a–h** is constructed by only type of $[LnO_8(H_2O)]$ polyhedra sharing edge *via* two –COO group bridges of glu ligands, while 1-D chain of **3** is based on two types of $[LaO_8(H_2O)_x]$ ($x = 1, 2$) polyhedra. (b) Different bridging modes of glu ligands: the structures of **4a–h** possess two types of bridging modes, namely one has two chelating –COO groups, the other has two chelating–*anti* –COO groups, whereas the structure of **3** has three kinds of bridging modes, where two –COO groups of each glu ligand adopt different coordination modes. (c) Different space groups and sizes of channels: **3** crystallizes in space group $P\bar{1}$ and has large rectangular channels that are filled by free water molecules, but **4a–h** crystallizes in space group $C2/c$ and has small circular channels, where free water molecules are incorporated.

Influence of lanthanide contraction. Lanthanide contraction is a term used in chemistry to describe the steady decrease in the size of Ln^{3+} ions with increasing atomic number, where the use of different lanthanide chlorides has dramatically influenced the solid-state architectures of lanthanide glutarates. The reactions of $LnCl_3$ salts and glu ligands in the presence of phen under similar hydrothermal conditions have given two types of lanthanide glutarates. The first type contains a repeating structure unit of the formula $[Ln(phen)(glu)Cl]$ [Ln = Y (**1a**), Tm (**1b**)], where the Ln^{3+} ions (Ln = Y, Tm) all eight-coordinated environment forming the polyhedra $[LnO_5N_2(H_2O)]$ surrounded by four glu ligands, one phen and one Cl^- anion, leading to the 1-D chains. The second type is composed of a repeating molecular composition $[Ln_2(phen)_2(glu)_3]$ {Ln = Ce (**2a**), Pr,[8a] Eu,[8a] Tb (**2b**), Ho (**2c**), Er[8a]}, where the coordination number of Ln^{3+} ions is nine, but each Ln^{3+} ion is bridged by five glu ligands and one phen, resulting in the 2-D layers. When the above reaction system reacted in the absence of phen, another two types of lanthanide glutarates were obtained. In **3**, the coordination number of largest La^{3+} ion can reach to 10, and La^{3+} ion can be surrounded by six glu ligands, but the coordination number of Ln^{3+} ion in $[Ln(glu)_3(H_2O)_2]_n \cdot 4nH_2O$ (Ln = Pr, Nd, Sm, Eu, Gd, Tb, Dy, Ho and Y)[7a–c] is nine and each Ln^{3+} ion is surrounded by five glu ligands. The results demonstrated that the well-known lanthanide contraction has a significant influence on the formation of lanthanide glutarates under hydrothermal conditions.

IR spectra and photoluminescent properties

The IR spectra of all compounds show the characteristic bands of the –COO$^-$ groups in the range of 1627–1517 cm^{-1} for $v_{C=O/C-O}$ asymmetric stretching and 1467–1343 cm^{-1} for $v_{C=O/C-O}$ symmetric stretching. The weak bands at 3094–3010 cm^{-1} in **1a–b** and **2a–c** belong to the v_{C-H} stretching of phen ligand, but no similar peaks in **3** appear, which further confirms the absence of phen ligand. The broad band at 3435 cm^{-1} can be attributed to v_{O-H} stretching of water molecules in **3**. Upon excitation at 345 nm, **1b** shows a broad band centered at 388 nm

(Fig. S5†). This band is attributed to the ligand emission due to its short lifetime (~15 μs obtained from its decay curve). The weak shoulder at 475 nm is assigned to the transition from the $^1G_4$ excited state to the $^3H_6$ ground state.

For **2b**, the excitation spectrum was obtained by monitoring the most intense emission wavelength of Tb^{3+} at 545 nm (Fig. 4a). It shows a broad band ranging from 240 to about 400 nm attributed to electronic transitions from the ground state level (π) S_0 to the excited level (π^*) S_1 of the organic ligand. The excitation spectrum also displays some weak sharp peaks at 326, 369, 378 and 487 nm assigned to Tb^{3+} ion intra f–f transitions $^7F_6 \rightarrow {}^5D_1$, $^7F_6 \rightarrow {}^5L_{10}$, $^7F_6 \rightarrow {}^5G_6$ and $^7F_6 \rightarrow {}^5D_4$, respectively. The dominate excitation bands are from the ligand, indicating that a sensitization of Tb^{3+} luminescence is mainly through an indirect energy transfer process from ligand to Tb^{3+} ions. Upon excitation at the most intensive wavelength 280 nm (Fig. 4b), the emission spectrum exhibits four strong emission bands at 489, 545, 586, and 622 nm corresponding to $^5D_4 \rightarrow {}^7F_J$ ($J = 6, 5, 4, 3$), and three weak bands located at 645, 668 and 679 nm arising from the $^5D_4 \rightarrow {}^7F_J$ ($J = 2, 1, 0$), respectively, with the $^5D_4 \rightarrow {}^7F_5$ emission as the dominant band. Since no emission bands from the ligand were observed, it is further demonstrated that there is an intramolecular energy transfer from the ligand to Tb^{3+} ions. The intensities of characteristic Tb^{3+} emissions are obviously stronger than those of $[Tb(H_2O)]_2(glu)_3 \cdot 4H_2O$,[7c] which contain the coordinated H_2O molecules. This result demonstrated that the introduction of chromophoric phen ligand into the frameworks of lanthanide glutarates can enhance the intensity of Ln^{3+} emissions. The luminescence decay curve of Tb^{3+} related to the $^5D_4 \rightarrow {}^7F_5$ emission (545 nm) was shown in Fig. 4c. The decay curve is singly exponential, confirming that all Tb^{3+} ions lie in the same average environment. The luminescence lifetime was determined to be 0.414 ms. The CIE chromaticity coordinate was calculated to be (0.35, 0.59), as shown in Fig. 4d.
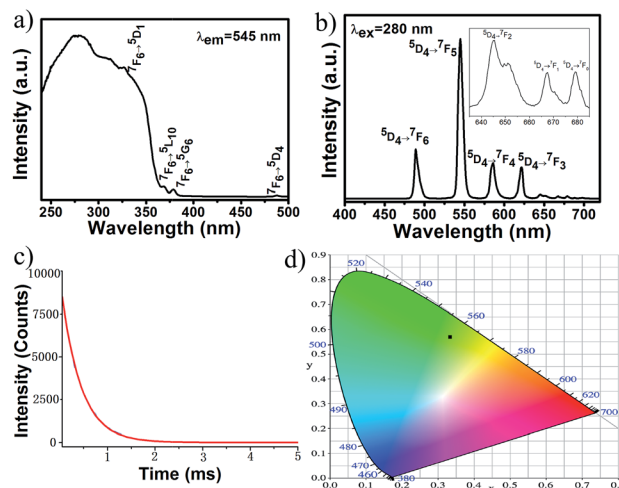

Fig. 4 (a) Excitation spectrum for **2b** (λ_{em} = 545 nm). (b) Emission spectrum for **2b** (λ_{ex} = 280 nm, the enlarged part shows the emission bands between 635 to 685 nm). (c) Decay curve for **2b**. (d) CIE chromaticity diagram for **2b** at λ_{ex} = 280 nm.

Paper

Magnetic properties

The magnetic susceptibilities of compounds **1b**, **2b** and **2c** were measured in the temperature range 2–300 K under an applied magnetic field of 1 kOe. For **1b**, the $\chi_M T$ value (7.37 cm^3 K mol^{-1}) at room temperature is close to the theoretical value for one non-interacting Tm^{3+} ion (7.08 cm^3 K mol^{-1} for Tm^{3+}, ^{3}H$_6$, $S = 1$, $L = 5$, $J = 6$, $g = 7/6$). With lowering temperature, $\chi_M T$ value shows a slight decrease for **1b** (Fig. 5a), as a result of as a consequence of the depopulation of sublevels of the ground J multiplet split by the crystal field[13] and possible antiferromagnetic interactions.[14] Antiferromagnetic interactions between Tm^{3+} ions can be also confirmed by the smaller Tm–O–Tm angle value of 106.97°, because the rule is that Ln–O–Ln angles below 113.50° are assumed to cause an antiferromagnetic exchange in the literature.[15] For **2b**, the $\chi_M T$ value at room temperature is 23.61 cm^3 K mol^{-1} (Fig. 5b), which is in good agreement with the expected theoretical values for two uncoupled Tb^{3+} ions (23.64 cm^3 K mol^{-1} for Tb^{3+}, ^{7}F$_6$, $S = 3$, $L = 3$, $J = 6$, $g = 3/2$). Upon cooling, $\chi_M T$ increases to a maximum of 26.33 cm^3 K mol^{-1} at 54 K. This magnetic behavior typifies the ferromagnetic coupling interactions between adjacent Tb^{3+} centers. A sudden decrease of the $\chi_M T$ value below 54 K suggests that is a consequence of the depopulation of sublevels of the ground J multiplet split by the crystal field and antiferromagnetic interactions. The ferromagnetic interactions provided by chelating–*anti* –COO bridges[2a] in the dimer could also be concomitant with significant antiferromagnetic interactions, due to the Tb–O–Tb angle values in the range of 104.54–107.54° below 113.50°. The classical *syn–anti* –COO bridges within the dimeric entity appear as the most likely pathways for the antiferromagnetic exchange.[2a]

For **2c**, the $\chi_M T$ value (28.46 cm^3 K mol^{-1}) at room temperature (Fig. 5c) is as expected for two magnetically isolated Ho^{3+} ion (28.14 cm^3 K mol^{-1} for Ho^{3+}, ^{5}I$_8$, $S = 2$, $L = 6$, $J = 8$, $g = 5/4$). As the temperature is lowered, this value remains practically constant until 28 K and it decreases further to reach a value of 2.46 cm^3 K mol^{-1} at 3 K. This plot can be indicative of the existence of an antiferromagnetic coupling between the Ho^{3+}

ions, which is further confirmed by the smaller Ho–O–Ho angle values of 103.81–107.58° below 113.50°.[15] The χ_M^{-1} *versus* T over the entire temperature range for compounds **1b**, **2b** and **2c** can be fitted to the Curie–Weiss law, $\chi_M = C/(T - \theta)$ with the Curie constant $C = 7.47$, 23.95 and 28.47 cm^3 K mol^{-1}, and the Weiss constant $\theta = -4.53$, 2.65 and -1.29, respectively (Fig. 5d).

Conclusions

A series of lanthanide glutarates were isolated as single crystals under mild hydrothermal conditions in the presence of phen. The lighter Ln^{3+} ions form the 2-D layers, while the heavier ones form the 1-D chains, where the change in their crystal architectures is obviously related to the well-known lanthanide contraction. The chromophoric phen ligand was incorporated successfully into the frameworks of lanthanide glutarates and prevents water molecules from binding to Ln^{3+} ions, which could lead to the enhancement of characteristic Ln^{3+} emissions, for instance, **2b** can emit stronger green luminescence at 545 nm with long luminescent lifetime, making **2b** a good candidate for potential green materials. Moreover, the interconnections of Ln^{3+} ions and glu ligands lead to very robust structural type $[Ln(glu)_3(H_2O)_2]_n \cdot 4nH_2O$, whose 3-D networks containing 1-D inorganic chains of edge-sharing $[LnO_8(H_2O)]$ polyhedra are not changed by different Ln^{3+} ions, but 3-D framework of **3** contains 1-D inorganic chains based on two types of $[LaO_8(H_2O)_x]$ ($x = 1$, 2) polyhedra, which exhibits a new structural type. The successful synthesis of lanthanide glutarates containing chromophoric phen ligand not only enriches the existing field of lanthanide coordination polymers but also opens possibilities for synthesizing other novel photoluminescent lanthanide glutarates using chromophoric phen derivatives units under desirable conditions.

Acknowledgements

Fig. 5 The plot of $\chi_M T$ versus T for **1b** (a), **2b** (b) and **2c** (c). (d) Plot of χ_M^{-1} *versus* T for **1b**, **2b** and **2c**.

Notes and references

1 (*a*) N. Ishikawa, T. Iino and Y. Kaizu, *J. Am. Chem. Soc.*, 2002, **124**, 11440; (*b*) G. Novitchi, W. Wernsdorfer, L. F. Chibotaru, J. Costes, C. E. Anson and A. K. Powell, *Angew. Chem., Int. Ed.*,
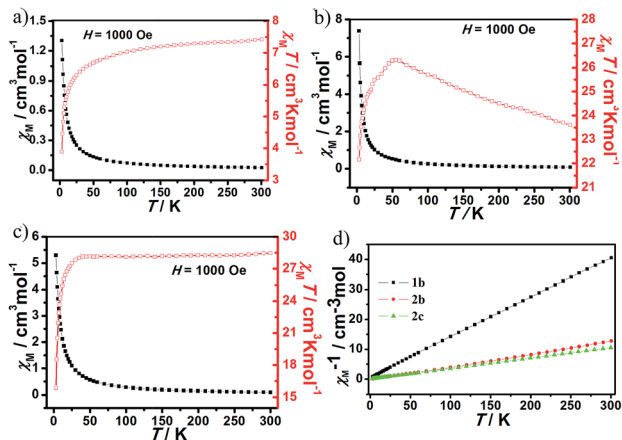
2009, **48**, 1614; (*c*) C. Benelli and D. Gatteschi, *Chem. Rev.*, 2002, **102**, 2369; (*d*) P. Lin, T. J. Burchell, R. Clérac and M. Murugesu, *Angew. Chem., Int. Ed.*, 2008, **47**, 8848; (*e*) J. Peng, X. Kong, Q. Zhang, M. Orendac, J. Prokleska, Y. Ren, L. Long, Z. Zheng and L. Zheng, *J. Am. Chem. Soc.*, 2014, **136**, 17938; (*f*) D. D'Alessio, A. N. Sobolev, B. W. Skelton, R. O. Fuller, R. C. Woodward, N. A. Lengkeek, B. H. Fraser, M. Massi and M. I. Ogden, *J. Am. Chem. Soc.*, 2014, **136**, 15122; (*g*) J. M. Clemente-Juan, E. Coronado and A. Gaita-Arino, *Chem. Soc. Rev.*, 2012, **41**, 7464.

2 (*a*) Y. Zheng, Z. Zheng and X. Chen, *Coord. Chem. Rev.*, 2014, **258–259**, 1; (*b*) P. Zhang, L. Zhang, C. Wang, S. Xue, S. Lin and J. Tang, *J. Am. Chem. Soc.*, 2014, **136**, 4484; (*c*) N. Ishikawa, M. Sugita and W. Wernsdorfer, *J. Am. Chem. Soc.*, 2005, **127**, 3650; (*d*) N. Ishikawa, T. Iino and Y. Kaizu, *J. Am. Chem. Soc.*, 2002, **124**, 11440; (*e*) A. B. Canaj, D. I. Tzimopoulos, M. Siczek, T. Lis, R. Inglis and C. J. Milios, *Inorg. Chem.*, 2015, **54**, 7089; (*f*) X. Tan, J. Zhou, L. Fu, H. Xiao, H. Zou and Q. Tang, *Dalton Trans.*, 2016, **45**, 5253.

3 (*a*) Y. Cui, B. Chen and G. Qian, *Coord. Chem. Rev.*, 2014, **273–274**, 76; (*b*) K. Binnemans, *Chem. Rev.*, 2009, **109**, 4283; (*c*) X. Yang, D. Schipper, R. A. Jones, B. J. Holliday, S. Huang and L. A. Lytwak, *J. Am. Chem. Soc.*, 2013, **135**, 8468; (*d*) J. Rausch, V. Lorenz, C. G. Hrib, V. Frettlöh, M. Adlung, C. Wickleder, L. Hilfert, P. G. Jones and F. T. Edelmann, *Inorg. Chem.*, 2014, **53**, 11662; (*e*) X. Feng, Y. Feng, J. J. Chen, S. Ng, L. Wang and J. Guo, *Dalton Trans.*, 2015, **44**, 804.

4 (*a*) G. Stein and E. Wurzberg, *J. Chem. Phys.*, 1975, **62**, 208; (*b*) Y. Haas and G. Stein, *J. Phys. Chem.*, 1971, **75**, 3677.

5 (*a*) L. N. Puntus, K. A. Lyssenko, I. S. Pekareva and J. G. Bünzli, *J. Phys. Chem. B*, 2009, **113**, 9265; (*b*) R. Martínez-Manez and F. Sancenón, *Chem. Rev.*, 2003, **103**, 4419; (*c*) X. P. Yang, R. A. Jones, M. M. Oye, A. L. Holmes and W.-K. Wong, *Cryst. Growth Des.*, 2006, **6**, 2122; (*d*) J.-C. G. Bünzli and C. Piguet, *Chem. Rev.*, 2002, **102**, 1897.

6 (*a*) X. Huang, Q. Wang, X. Yan, J. Xu, W. Liu, Q. Wang and Y. Tang, *J. Phys. Chem. C*, 2011, **115**, 2332; (*b*) Y. Hasegawa, S. Tsuruoka, T. Yoshida, H. Kawai and T. Kawai, *J. Phys. Chem. A*, 2008, **112**, 803; (*c*) P. Lenaerts, A. Storms, J. Mullens, J. D'Haen, C. Görller-Walrand, K. Binnemans and K. Driesen, *Chem. Mater.*, 2005, **17**, 5194; (*d*) X. Ma, X. Li, Y. Cha and L. Jin, *Cryst. Growth Des.*, 2012, **12**, 5227;

(*e*) L. N. Puntus, K. A. Lyssenko, M. Y. Antipin and J. G. Bünzli, *Inorg. Chem.*, 2008, **47**, 11095.

7 (*a*) E. Antic-Fidancev, F. Serpaggi and G. Férey, *J. Alloys Compd.*, 2002, **340**, 88; (*b*) F. Serpaggi and G. Férey, *J. Mater. Chem.*, 1998, **8**, 2737; (*c*) B. Yu, C. Xie, X. Wang, R. Wang, G. Shen and D. Shen, *J. Coord. Chem.*, 2007, **60**, 1817; (*d*) C. Wang, Y. Xing, Z. Li, J. Li, X. Zeng, M. Ge and S. Niu, *J. Mol. Struct.*, 2009, **931**, 76; (*e*) P. I. Girginova, F. A. Almeida Paz, P. C. R. Soares-Santos, R. A. Sá Ferreira, L. D. Carlos, V. S. Amaral, J. Klinowski, H. I. S. Nogueira and T. Trindade, *Eur. J. Inorg. Chem.*, 2007, 4238; (*f*) Y. Kim, Y. Park and D. Jung, *Dalton Trans.*, 2005, 2603; (*g*) A. Dimos, D. Tsaousis, A. Michaelides, S. Skoulika, S. Golhen, L. Ouahab, C. Didierjean and A. Aubry, *Chem. Mater.*, 2002, **14**, 2616.

8 (*a*) D. Wei, H. Xie, S. Huang, J. Zhou and G. Lu, *J. Coord. Chem.*, 2011, **64**, 424; (*b*) L. Zhang, Y. Wan and L. Jin, *J. Mol. Struct.*, 2003, **646**, 169.

9 (*a*) G. M. Sheldrick, *SHELXS-97, Program for the Solution of Crystal Structures*, University of Göttingen, Göttingen, Germany, 1997; (*b*) G. M. Sheldrick, *Acta Crystallogr., Sect. A: Found. Crystallogr.*, 1990, **46**, 467.

10 (*a*) G. M. Sheldrick, *SHELXL-97, Program for the Refinement of Crystal Structures*, University of Göttingen, Göttingen, Germany, 1997; (*b*) G. M. Sheldrick, *Acta Crystallogr., Sect. A: Found. Crystallogr.*, 2008, **64**, 112.

11 (*a*) K. P. Carter, S. J. A. Pope and C. L. Cahil, *CrystEngComm*, 2014, **16**, 1873; (*b*) C. Wang, Z. Wang, F. Gu and G. Guo, *J. Mol. Struct.*, 2010, **979**, 92.

12 F. Bai, J. Xu, H. Su and X. Gu, *Z. Anorg. Allg. Chem.*, 2012, **638**, 2366.

13 (*a*) Y.-L. Wang, Y. Ma, X. Yang, J.-K. Tang, P. Cheng, Q.-L. Wang, L.-C. Li and D.-Z. Liao, *Inorg. Chem.*, 2013, **52**, 7380; (*b*) H.-S. Ke, G.-F. Xu, Y.-N. Guo, P. Gamez, C. M. Beavers, S. J. Teat and J.-K. Tang, *Chem. Commun.*, 2010, **46**, 6057.

14 (*a*) G. Abbas, Y. H. Lan, G. E. Kostakis, W. Wernsdorfer, C. E. Anson and A. K. Powell, *Inorg. Chem.*, 2010, **49**, 8067; (*b*) J. Zhou, R. Zhao, T. Yang, X. Liu, H. Xiao, H. Zou and X. Tan, *Dalton Trans.*, 2015, **44**, 7203; (*c*) J. Zhou, H. Xiao, H. Xiao, T. Yang, H. Zou, X. Liu, R. Zhao and Q. Tang, *Dalton Trans.*, 2015, **44**, 1350.

15 B. Benmerad, K. Aliouane, N. Rahahlia, A. Guehria-Laïdoudi, S. Dahaoui and C. Lecomte, *J. Rare Earths*, 2013, **31**, 85.